
Intra-agent speech permits zero-shot task acquisition

Chen Yan
DeepMind
London, UK
ywc@deepmind.com

Federico Carnevale
DeepMind
London, UK
fedecarnev@deepmind.com

Petko Georgiev
DeepMind
London, UK
petkoig@deepmind.com

Adam Santoro
DeepMind
London, UK
adamsantoro@deepmind.com

Aurelia Guy
OpenAI
San Francisco, USA
7aureliaguy@gmail.com

Alistair Muldal
DeepMind
London, UK
alimuldal@deepmind.com

Chia-Chun Hung
Isomorphic Labs
London, UK
aldenhung@google.com

Josh Abramson
DeepMind
London, UK
jabramson@deepmind.com

Timothy Lillicrap
DeepMind
London, UK
countzero@deepmind.com

Gregory Wayne
DeepMind
London, UK
gregwayne@deepmind.com

Abstract

Human language learners are exposed to a trickle of informative, context-sensitive language, but a flood of raw sensory data. Through both social language use and *internal* processes of rehearsal and practice, language learners are able to build high-level, semantic representations that explain their perceptions. Here, we take inspiration from such processes of “inner speech” in humans (Vygotsky, 1934) to better understand the role of *intra-agent speech* in embodied behaviour. First, we formally pose intra-agent speech as a semi-supervised problem and develop two algorithms that enable visually grounded captioning with little labeled language data. We then experimentally compute scaling curves over different amounts of labeled data and compare the data efficiency against a supervised learning baseline. Finally, we incorporate intra-agent speech into an embodied, mobile manipulator agent operating in a 3D virtual world, and show that with as few as 150 additional image captions, intra-agent speech endows the agent with the ability to manipulate and answer questions about a new object without any related task-directed experience (zero-shot). Taken together, our experiments suggest that modelling intra-agent speech is effective in enabling embodied agents to learn new tasks efficiently and without direct interaction experience.

1 Introduction

Contemporary language models learn from troves of text comprising billions, and sometimes trillions of tokens. This is not the same situation faced by embodied language learners, such as human children, whose raw sensory data vastly exceeds their social-linguistic experiences. Psychologists have long noted the existence of non-social, intra-personal dialogue—such as inner speech (silent) or private

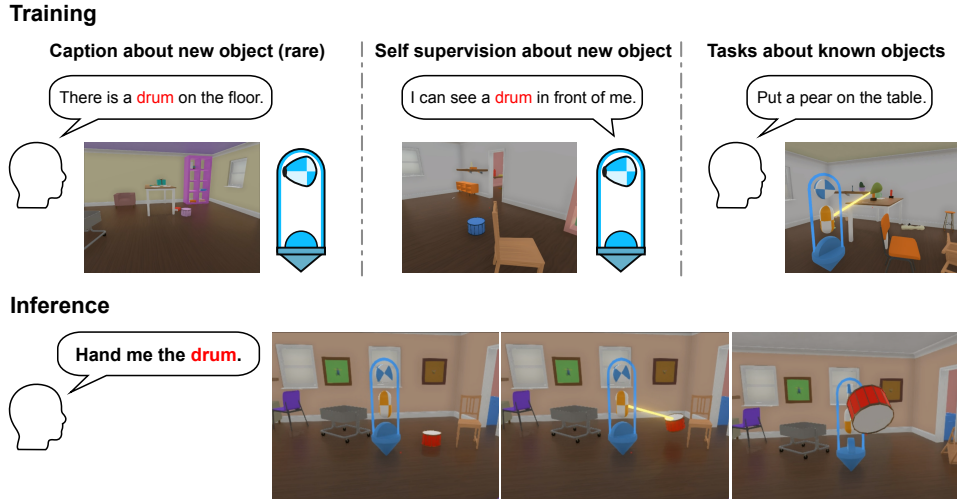


Figure 1: Learning to speak about new objects permits zero-shot motor task behavior. Is it possible for agents to perform complex tasks with a new object just by learning to name it? In this work, we show it is. We first trained agents to speak about objects that had never been used in any task, nor named in any interaction, by training agents to caption their observations (top row, left and middle). We then introduced interactive tasks involving other objects and trained agents with imitation learning (top right). Using only a small number of labeled captions that pertained to a new object category (drums), agents were able to perform tasks involving the new objects, such as lifting and delivering them to a second avatar (bottom).

speech (aloud)—which provides additional linguistic experiences beyond those encountered in social settings. Indeed, one possible reason for intra-personal speech may be to support the development of social speech [1–5], though the inverse causal relation may also be possible [1, 6].

Intra-personal speech may also affect broader aspects of our cognition: the process wherein we privately speak about our perceptions subsequently impacts how we attend to, remember, or manipulate the objects of our perception [7–12]. For example, our short-term memories tend to commit errors for items that are phonetically but not visually or semantically similar [8, 9], and “self-talk” affects task performance on executive tasks both in children [11, 12] and in adults [7], and has been widely used to improve athletic performance [10].

Inspired by these ideas, here we ask if we can leverage *intra-agent speech* as a tool for artificial intelligence research. Specifically, we ask the following questions: First, is it possible to model intra-agent speech as a machine learning problem, enabling us to make up for a paucity of language data when given access to a large amount of unlabeled data? Second, can mechanisms for learning intra-agent speech impact the subsequent behavior of an embodied agent?

Regarding the first, we formally structure intra-agent speech as a semi-supervised problem. In particular, we model intra-agent speech samples as variational latent variables representing images, and use this perspective to devise two algorithms enabling visual captioning given a paucity of directly labeled data. Regarding the second, we go on to show how embedding such algorithms in an embodied agent not only permits the capacity to speak about any given perception (that is, *to caption*, which is precisely what is being optimized for) but rather also permits zero-shot behaviors involving new objects that were never directly implicated in any task-directed experience (see Figure 1).

2 Approach

At a high level, we structured intra-agent speech as the production of language generated from inputs (which in our case manifests as captions of images), with two additional concerns: First, there will be a preponderance of unlabeled data (i.e., pure images) relative to labeled data (i.e., images with associated captions) in our captioning dataset, much like the situations faced by human children in nature and semi-supervised learning in machine learning. Second, the linguistic representations eventually produced will provide auxiliary supervision for an embodied, acting agent so that they may influence interactive behavior.

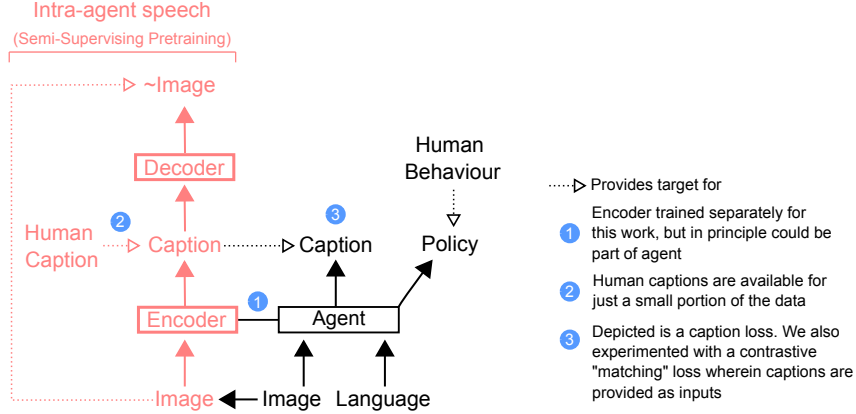


Figure 2: Using models of intra-agent speech to influence behavior. During intra-agent speech pre-training, agents receive image observations as input and produce either utterances that describe the observations (for the small number of inputs for which we have human annotated labels) or are tasked with reconstructing the images (using a generative model whose latent representations comprise language tokens). During behavioral training, the intra-agent speech module is frozen and is used to provide targets for an auxiliary captioning loss, whose gradients affect components responsible for action selection.

While in humans both inner speech and behavior develop simultaneously, here the system is trained in two stages for simplicity. First, we develop a semi-supervised language learning method to efficiently pre-train a capacity for intra-agent speech when given access to large amounts of unlabeled data and small amounts of labeled language data. We then explore how this capacity for intra-agent speech can be leveraged to shape subsequent interactive behavior in an embodied agent. A diagram of the semi-supervised learning approach to intra-agent speech and its role in acquiring behaviors is shown in Figure 2.

2.1 Methods for Semi-supervised Language Learning

Our data D are composed of a dataset D_p of paired data $\{\mathbf{x}, \mathbf{y}\}$ and a dataset D_u of unpaired data $\{\mathbf{x}\}$. In our interpretation, \mathbf{y} corresponds to language (a caption) describing the image \mathbf{x} . When observing unpaired data, we treat \mathbf{y} as a latent variable that must be inferred to explain the observed data [13]. We develop two variants, one generative and one contrastive, of the semi-supervised language learning algorithm in what follows.

2.1.1 Generative variant

The preponderance of our data is unlabeled. To model these data we can maximise a variational lower bound on the log marginal distribution, $\log p_\theta(\mathbf{x})$, corresponding to posterior inference. We will use a learned approximation to the true posterior distribution, $q_\omega(\mathbf{y} | \mathbf{x})$. We call this approximate distribution an “image-conditional language encoder” (or sometimes, simply, *caption model*) since its functional role is to convert images into a discrete latent code that is, ideally, a semantically meaningful language caption:

$$\sum_{\mathbf{x} \sim D_u} \log p_\theta(\mathbf{x}) \geq \sum_{\mathbf{x} \sim D_u} \mathbb{E}_{q_\omega(\mathbf{y} | \mathbf{x})} [\log p_\theta(\mathbf{x} | \mathbf{y})] - \mathcal{D}_{\text{KL}}[q_\omega(\mathbf{y} | \mathbf{x}) \| p_\phi(\mathbf{y})] \quad (1)$$

$$= J_u.$$

In Equation 1, the space of latent codes (captions) is discrete and vast, complicating optimization. However, we can form a stochastic approximation by sampling from $q_\omega(\mathbf{y} | \mathbf{x})$ to estimate a gradient.

$$\nabla_\omega J_u = \sum_{\mathbf{x} \sim D_u} \mathbb{E}_{q_\omega(\mathbf{y} | \mathbf{x})} [\nabla_\omega \log q_\omega(\mathbf{y} | \mathbf{x}) (\log p_\theta(\mathbf{x} | \mathbf{y}) + \log p_\phi(\mathbf{y}) - \log q_\omega(\mathbf{y} | \mathbf{x}))]. \quad (2)$$

For simplicity, we pretrain the prior $p_\phi(\mathbf{y})$ as a language model that learns on all of our caption data, and fix it during this optimisation phase. Thus, optimising J_u corresponds to an entropy-regularised

RL problem [14–16]. The encoder $q_\omega(\mathbf{y} | \mathbf{x})$ serves as a policy that achieves reward for matching the language model prior while enabling the language-conditional decoder to reconstruct the image.

While this reward pressures the image-conditional language encoder to produce linguistically meaningful latent codes, we can also exert additional pressure by using a small number of images with associated captions (“labeled data”), and leverage supervised learning to learn $\log p_\theta(\mathbf{x} | \mathbf{y}), \log p_\phi(\mathbf{y}), \log q_\omega(\mathbf{y} | \mathbf{x})$:

$$J_p = \sum_{\mathbf{x}, \mathbf{y} \sim D_p} [\log p_\theta(\mathbf{x} | \mathbf{y}) + \log p_\phi(\mathbf{y}) + \log q_\omega(\mathbf{y} | \mathbf{x})]. \quad (3)$$

Over the combined paired and unpaired datasets, our complete objective is to maximise $J = J_p + J_u$.

2.1.2 Contrastive variant

The language-conditional image decoder $p_\theta(\mathbf{x} | \mathbf{y})$ is a potentially complicated term to model. To understand if this term represents a liability for the approach and to generate an algorithm with potentially complementary strengths, we also developed a contrastive, energy-based approach, amounting to multi-class classification, to approximate it [17–19]. If we have a multi-class classifier that discriminates if a batch element \mathbf{y}_j is paired to a batch element \mathbf{x}_j , and we express its cross-entropy loss for the correct index $c = j$ as $L(\{\mathbf{x}_b\}_{b=1}^B, \mathbf{y}_j, c = j)$, then we can show that the generative reconstruction loss $\log p_\theta(\mathbf{x}_j | \mathbf{y}_j)$ is proportional to $L(\{\mathbf{x}_b\}_{b=1}^B, \mathbf{y}_j, c = j)$ up to constant factors with respect to \mathbf{y} (Appendix A.1). Thus, we can substitute $L(\{\mathbf{x}_b\}_{b=1}^B, \mathbf{y}_j, c = j)$ for batch element j , $\log p_\theta(\mathbf{x}_j | \mathbf{y}_j)$, in Equation 2, and the gradients with respect to ω remain the same in expectation.

We represented the softmax in the classifier as $\frac{e^{\mathbf{f}(\mathbf{x}_j)^\top \mathbf{g}(\mathbf{y}_j)}}{\sum_{b=1}^B e^{\mathbf{f}(\mathbf{x}_b)^\top \mathbf{g}(\mathbf{y}_j)}}$, where \mathbf{f} and \mathbf{g} are networks that compress the image into a vector and the caption into a vector, respectively. To train this classifier, we adopted a similar approach to recent models for visual language representation learning [20, 21] by minimizing the sum of two losses, one for matching each image to its paired caption in the batch, and one for matching each caption to its paired image:

$$L = \frac{1}{B} \sum_{j=1}^B \log \frac{e^{\mathbf{f}(\mathbf{x}_j)^\top \mathbf{g}(\mathbf{y}_j)}}{\sum_{b=1}^B e^{\mathbf{f}(\mathbf{x}_b)^\top \mathbf{g}(\mathbf{y}_j)}} + \frac{1}{B} \sum_{j=1}^B \log \frac{e^{\mathbf{f}(\mathbf{x}_j)^\top \mathbf{g}(\mathbf{y}_j)}}{\sum_{b=1}^B e^{\mathbf{f}(\mathbf{x}_j)^\top \mathbf{g}(\mathbf{y}_b)}} \quad (4)$$

The networks \mathbf{f} and \mathbf{g} are trained at the same time as the rest of the model, and samples from $q_\omega(\mathbf{y}_j | \mathbf{x}_j)$ are included as positive examples for the classifier along with the original paired data.

2.1.3 Intra-agent speech architecture and optimization

Image-conditional language encoder. The image-conditional language encoder received input images with resolution 96×72 . We used the ResNet architecture described in [22], with strides (1, 1, 2, 2), 3×3 kernel size, and channel sizes (64, 64, 128, 256) for a total of 20 layers. Language was produced by a 4-layer causal transformer with 256 embedding size and 4 attention heads [23], which attended to the 432 hyper-pixel vectors generated from the ResNet, and produced a sequence of logits corresponding to a 4,000 token vocabulary. Language targets were encoded with a SentencePiece byte-pair encoder [24] trained using language data from [25].

Generative semi-supervised model. The language prior comprised a separate transformer pre-trained on all the caption labels in the training data (and hence, did not have image inputs). For the image decoder, we first pre-trained a VQ-VAE [26] on all unlabeled images to define the VQ-VAE’s codebook, compressing each image into 432 tokens with a vocabulary of 512. We then used an 8-layer transformer with 512 embedding size with causal masking to model the VQ-VAE tokens autoregressively. The conditioning captions were tokenized and embedded as in the image-conditional language encoder, and then processed by a distinct transformer with 4 layers, 256 embedding size, and 4 heads, whose output was then cross-attended by the image decoder to produce a reconstruction.

Contrastive semi-supervised model. For the contrastive model, images were first encoded using a ResNet with the same architecture as the image-conditional language encoder, and globally mean-pooled into one vector with dimension 1024. Language was first encoded using a transformer with

the same 4-layer architecture described above, and then flattened and compressed with a 2-layer MLP with dimensions (2048, 1024).

Optimization. We used V-MPO [16] to optimize $q_\omega(\mathbf{y} | \mathbf{x})$. The loss was optimized by the Adam optimizer [27] with $\beta_1 = 0.9, \beta_2 = 0.999$ and a learning rate of 2×10^{-4} with early stopping at the lowest log-likelihood over captions in validation data. We trained all models with a batch size of 128 except for the contrastive classifier model, which also received 2,048 unlabeled images per batch, giving a total batch size of 2,176. We trained our models using Tensor Processing Units (TPUv3) [28]. In all experiments the early stopping criteria was reached within 150K optimization steps.

2.2 Agent training

The agent was trained by behavioral cloning on a large corpus of human interactions in the Playhouse environment [22]. Briefly, it comprises a 3D simulated environment wherein two embodied avatars interact with natural language to cooperatively accomplish tasks involving object manipulation, navigation, and question answering. In addition to receiving visual observations and producing motor actions, agents in this environment also receive language inputs and produce language outputs. This allows them to answer questions, participate in dialogue, ask for clarifications, and so on.

Our approach to training the linguistic representations of the agent therefore has two steps. First, by using semi-supervised language learning, we can amplify the impact of sparse language annotations provided for a small number of images in learning the intra-agent speech module. In turn, using this trained module, we are able to sample captions at high frequency as the agent acts, providing the agent with dense language supervision. Therefore, while the agent trains using behavioral cloning, we can sample captions from the pretrained intra-agent speech module, and provide these as either auxiliary inputs or targets to the agent so that they may influence the agent parameters optimized to produce embodied behaviors.

For our first loss – the caption loss – captions arising as intra-agent speech samples were provided as targets for the agent’s language output policy:

$$L_C = -\frac{1}{B} \sum_{b=1}^B \sum_{t=0}^K \ln \pi_l(\mathbf{y}_{b,t}^c | \mathbf{o}_{b,\leq t}), \quad (5)$$

where π_l is the language action policy of the agent, \mathbf{y}^c is the caption sample, \mathbf{o} represents all visual and text observations, and K represents the maximum unroll length. To allow the agent to distinguish whether it was being tasked with emitting a caption of its current observation, or whether it was being tasked with emitting language for the purposes of interactive behavior (see [22]), the agent also received a corresponding binary indicator embedding as input.

While the caption loss trains the agent to speak about what it sees, the agent’s language encoding (via linguistic inputs) remains untrained. To this end we introduced a second loss: the caption-matching loss. In the caption-matching loss, the agent is required to predict whether a given caption, provided as input, matches the observed image. Negative samples (i.e., captions that do not match the observation) are captions associated with images from elsewhere in the batch [29]. To perform this prediction, an auxiliary classifier D is attached to the network of the agent that encodes both visual and text observations in a separate training pass from the behavioral cloning optimization.

$$L_{CM} = -\frac{1}{B} \sum_{b=1}^B \sum_{t=0}^K \left[\ln D(\mathbf{o}_{b,t}^X, \mathbf{y}_{b,t}^c) + \ln (1 - D(\mathbf{o}_{b,t}^X, \mathbf{y}_{\text{roll}(b),t}^c)) \right]. \quad (6)$$

Here \mathbf{o}^X represents the visual observation, and the caption sample is fed as a text observation. The $\text{roll}()$ function rolls the index over batches, so that $\mathbf{y}_{\text{roll}(b)}^c$ represents a caption from another batch element as a negative example. The roll function was implemented as $\text{roll}(b) = (b + 1) \bmod B$.

And finally, the behavioral cloning loss over human language and movement action sequences is as described in Interactive Agents Team [22]:

$$L_{BC} = -\frac{1}{B} \sum_{b=1}^B \sum_{t=0}^K \left[\ln \pi_l(\mathbf{a}_{b,t}^l | \mathbf{o}_{b,\leq t}) + \ln \pi_m(\mathbf{a}_{b,t}^m | \mathbf{o}_{b,\leq t}) \right], \quad (7)$$

where the π_m and \mathbf{a}^m represents the movement policy and action, respectively.

The total loss is the sum of these losses $L = L_C + L_{CM} + L_{BC}$. Other than the addition of the caption loss and caption-matching loss, we follow Interactive Agents Team [22] for the agent architecture and training hyper-parameters.

3 Experiments

3.1 Semi-supervised captioning

Hypothesis. We first sought to validate our method of semi-supervised learning. We hypothesized that with the additional unlabeled images, the semi-supervised model would be more data efficient (with respect to labelled data) than a supervised baseline.

Data. As mentioned, the domain in which we tested our methods is called the Playhouse, which originated in Interactive Agents Team [22]. The authors compiled approximately three years worth of interaction data, comprising about 2 billion image frames. The authors have confirmed no personally identifiable information or offensive content is contained in the dataset and gave consent for us to access it. As there are no associated captions with any frames, we treat each frame in this dataset as a single image, and used all the data as our “unpaired” dataset.

For the “paired” dataset, we engaged with crowd raters to provide corresponding captions for 78K uniformly sampled images from the unpaired dataset. Raters were instructed to describe what they saw in the image, with particular reference to a randomly selected object indicated in a bounding box. Detailed instructions are included in Appendix A.2.

Evaluation. We measured the log probability of captions in the validation set, CIDEr score [30] and “color-object accuracy”. As the images were generated from the Playhouse environment, we had access to the ground truth object identities and colors present in each image, allowing us to check if color-object pairs mentioned in a caption were indeed present in the image. We calculated color-object accuracy to be the proportion of correct color-object pairs among all mentioned in sampled captions, normalized by the same calculation from human captions. As there are usually many objects in an image and captions tend to mention just a few, the recall counterpart of this metric (number of correct color-object pairs divided by those present in the image) is not very informative. Captions were greedily sampled for the calculation of CIDEr score and color-object accuracy.

Results. Figure 3 shows sample data used to train the our models, as well as samples generated from the generative semi-supervised model. Models were able to both produce coherent and relevant captions given an image (e.g., “I can see a white bed where a green ball and a green duck are on it”) and also generated realistic visual depictions of the Playhouse when conditioned on a language description.

Both semi-supervised methods performed better than the supervised baseline across all metrics, including settings where we artificially constrained the size of the labeled dataset (Figure 4). Notably, when using the full amount of data our semi-supervised methods exceeded human color-object accuracy. To further put the performance gain in context, by leveraging the unpaired dataset of images the semi-supervised methods performed at a level equivalent to training a supervised model on $3 \times$ more labeled data [31].

3.2 Learning captions of new objects

Hypothesis. Upon validating our methodology and amassing the relevant data, we were well-poised to ask the following questions: do semi-supervised methods of intra-agent speech allow a model to quickly learn to speak about a new object with little supervision?

Data. To address the hypothesis, we first chose an object – a *drum* – and filtered our labeled caption data to remove all instances where the drum is either depicted visually or spoken about verbally. While not strictly necessary, from the unlabeled dataset we also removed all instances where the underlying (and unobserved) instruction included mention of a drum, which ensured that all instances of drum appearances were truly “passive”. For example, the unlabeled data may have included trajectories of experience wherein a players was tasked with removing a ball from a shelf, but there might have also happened to be a drum in view in the room.

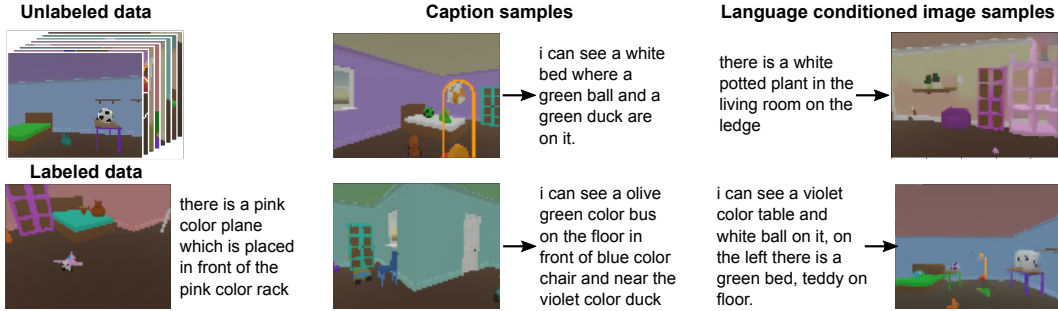


Figure 3: Data and Model Samples. Depicted are data used to train the semi-supervised model (left) and samples from the caption model (middle) and generative image model (right). As seen from the captions, generative modeling of images using a pre-trained language prior, in conjunction with auxiliary supervised training on a small number of labeled samples, is sufficient to produce meaningful and relevant language captions of images. Moreover, the model is able to generate realistic-looking scenes from provided captions. See Appendix A.3 for more samples.

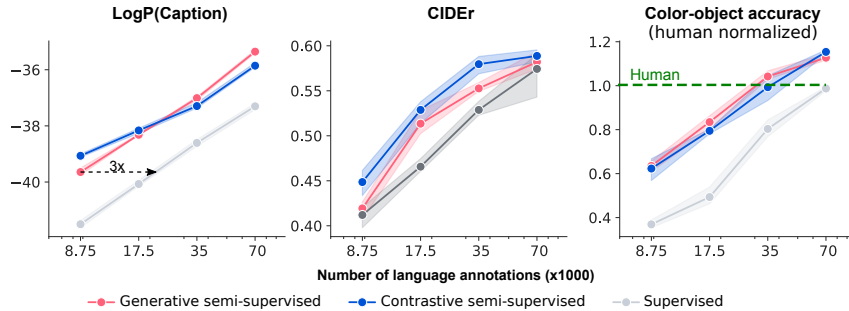


Figure 4: Scaling performance of semi-supervised models over labeled dataset sizes. Semi-supervised methods are trained with unlabeled data and titered amounts of labeled image-caption pairs. Here we calculate the log probability of validation set captions, the CIDEr score [30] and color-object accuracy. Color-object accuracy is calculated as the number of correct color-object pairs mentioned in the model caption samples divided by total number of color-object pairs mentioned in the caption. The same is calculated with human ground truth captions and the final score is calculated by the ratio of model over human color-object accuracy. Both semi-supervised models reach performances that equal that of the supervised model trained with 3x the data, and exceed human performance in color-object accuracy. Shading represents 95% confident intervals estimated from 3 random seeds for each data point.

Evaluation. We evaluated the model using three different metrics. We first created a validation dataset of all captions mentioning drum with their associated image, and evaluated the model’s average log likelihood on this drum dataset (drum caption log likelihood). The drum true positive rate, which is the probability that it mentions a drum given that a drum is present, measures how the model recognizes drums in the images. We also calculate its counterpart, the probability of the model erroneously mentioning a drum when it is not present as the drum false positive rate.

Results. We then performed the same experiment as in Section 3.1 at varying levels of re-introduced labeled drum data, as seen in Figure 4. As expected, the model’s ability to speak about drums scales with the amount of labeled drum data with which it is trained. Notably, the model’s true positive rate reaches approximately 70% given only 585 labeled samples of drums. In contrast, the supervised method reaches just over 20%. This indicates that the semi-supervised methods are able to learn about new objects, *implicitly*, by virtue of their language-conditioned reconstruction objective. That is, the mere presence of drums in the visual observations was sufficient, in conjunction with a small amount of labeled drum captions, to elicit linguistic understanding of drums as relevant objects in the Playhouse.

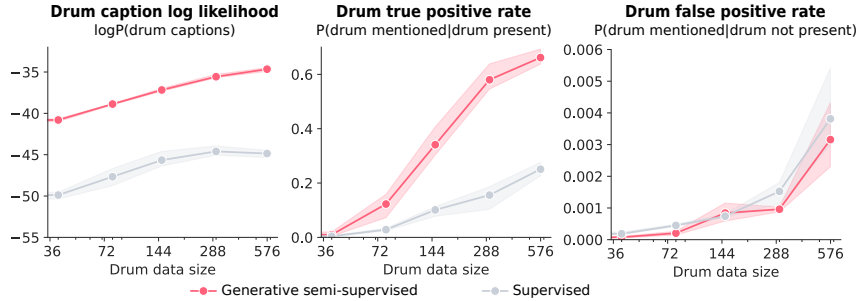


Figure 5: Scaling performance of our semi-supervised methods over drum dataset sizes. We examined how the semi-supervised and supervised methods scaled across different amounts of labeled data for a novel object. The semi-supervised trained model had a higher log likelihood, was more likely to recognize a drum in the image (high true positive rate) while displaying a comparable error-rate (same false positive rate). Extrapolating from supervised true positive rate, the supervised method would need more than $300\times$ more data to reach the same performance as the semi-supervised model. Shades represent 95% confident interval estimated from 3 random seeds for each data point.

3.3 Learning to manipulate a new object

Hypothesis. As a final test we tackled the final question: Can the ability to quickly learn to speak about an object confer advantages for learning behaviors involving the new object (such as manipulating the object, or answering questions about it)?

Methods and data. To answer this question we leveraged the semi-supervised models built in Section 3.2 to provide auxiliary intra-agent speech objectives. While we employed a two-stage process (learning to caption, and subsequently learning from those captions to shape behavior) for expedience and ease of experimental setup, in principle the two learning procedures could occur in parallel in a unified agent. The agent then proceeded with behavioral cloning-based training as in Interactive Agents Team [22] on data that was filtered *to not include* any drum-based instructions (resulting in 9,344 removed interactions).

Evaluation. We evaluated agent performance on two tasks: in the "lift drum" task, the agent receives the instruction "lift a drum", and is required to find the drum in a randomized Playhouse environment and lift it. In the "ask color drum" task, a single drum is spawned in the environment. The agent receives the instruction "what is the color of the drum?", and is then required to output language that answers the question (See Appendix A.4 for details). We collected human performance on each of the tasks and normalized reward by the average human score (note that rewards are used for evaluation purposes only, and not for training).

Results. As seen in Figure 6, a baseline agent trained without any drum-based instructions performs poorly on drum-based evaluation tasks, indicating that there is minimal transfer to be had when learning from the base interaction dataset. On the other hand, a model trained with drum-based instructions (that is, one that trains on the 9,344 episodes that we had filtered) displays an expected upper bound for this agent of just over 75% on "lifting drums", and just under 80% for answering questions about a drum's color, similar to previously reported results [22].

Agents trained with both the caption loss and caption-matching loss, but *without any drum-based interaction data* achieve approximately 70% of the performance attained by models trained directly on drum-based interaction data. This is a substantial increase over the baseline model, and directly indicates that learning to speak about drums, which is afforded by training a model on as few as 585 labeled drum examples using semi-supervised methods, allows an agent to subsequently exhibit behaviors that implicate the manipulation or mention of drums, without affecting performance on a known object (Appendix A.5).

We then tested whether we could reduce the number of labeled captions even further, and observed that with as few as 150 labeled captions we observed similar performance on drum-color question answering tasks, and only a slight decrease in drum lifting task performance.

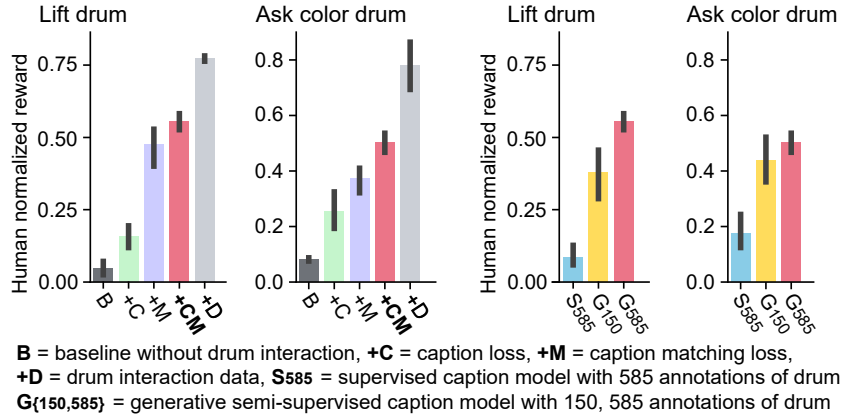


Figure 6: Zero-shot task-directed interaction with a novel object. We evaluated agent performance on two tasks that require interaction with the novel object (drum): in the first, the agent was tasked to locate and lift a drum, and in the second, the agent is required to mention the color of the drum using language. Our model with both the caption loss and caption matching loss (+CM) reaches more than 0.5 human normalized reward, comparable to approximately 70% of the performance of an agent trained with an additional 9344 episodes of interaction data including drums (+D; left two panels). This result also suggests the crucial role of semi-supervised training in zero-shot generalization (right two panels): with just 150 labeled captions of drum (G150), our model only displays a slight decrease in performance, but still significantly outperforms the supervised model trained on all the labelled captions (S585). Errorbars represent 95% confident interval estimated from 3 random seeds for each data point.

4 Related Work

Components. The modeling in this study builds on components developed for generative modeling (VQVAE-2: [32]) and contrastive learning (CLIP: [20]).

Task generalization in embodied agents. Our work is in the tradition of grounded language research in virtual environments [33–35]. Recently, there have been efforts to demonstrate zero-shot task acquisition using a variety of means including with the use of pretrained models for language encoders [36] or visual-language models for zero-shot navigation [37]. The majority of these works have focused on generalization to novel phrasings of task instructions [38, 39] with some recent studies exploring generalization to new tasks given background knowledge from previous tasks [22, 40]. Similar to phenomena of zero-shot generalization in supervised classification and object detection [20, 21, 41], these studies have often relied on a large, diverse dataset providing supervision – where held-out tasks represent a novel recombination of parts of the training dataset (e.g., “compositional” generalization or systematicity [42]). Another line of research has focused on few-shot generalization [43–46] through meta-learning over a distribution of tasks – with generalization to other tasks within the distribution’s support. Our work is complementary to both lines of work – and presents a means by which a different learning objective can embody “mental practice” enabling generalisation.

Semi-supervised learning with natural language. The semi-supervised methods we used to train the intra-agent speech module are related to many previous methods that use language as a latent variable. For example, Kingma et al. [13] developed a semi-supervised, variational autoencoder (VAE) with discrete latent variables, and this work has also been extended to use language as the latent variable. VAEs with language latent variables have also been studied in language summarization [47], and in the context of multi-agent communication with natural language [48, 49]. Our work may present a valuable contribution to this area, showcasing the utility of modern generative and contrastive models in supporting data-efficient learning. Our work’s analysis of the scaling curve [31] properties of semi-supervised captioning [50–52] may provide additional analytical tools for the field.

Language-conditioned image generation. The use of language to create sophisticated, controllable generative models has seen rapid development in recent years. Recent works based on diffusion models [53–55] and autoregressive models have produced some of the most impressive results. Notable work includes the DALL-E family of models [56, 57] and GLIDE [58]. Other work in the area has also employed VAEs [59] and GANs [60–64].

5 Conclusions and Future Work

In this work we built a model for intra-agent speech by leveraging semi-supervised learning techniques that maximize the impact of a small number of labeled samples in a sea of unlabeled samples. We further demonstrated how such models can help embodied agents execute interactive tasks without having to learn from direct interactive experience (zero-shot).

Although we developed the method in a virtual environment, it can be easily generalized to real world applications, applied with either good or bad intent. Embodied language agents acting as robots could be instructed to perform a wide manner of tasks, including harmful ones. Thus, if this work is to be applied in real settings, we advise extra caution to minimize unintended or harmful consequences.

This work is a first step into leveraging ideas from the psychology of inner and private speech in humans. While our source of speech was captioning, humans have a richer repertoire of techniques for intra-personal dialogue that affect modalities beyond vision. Direct next steps are, therefore, to explore a possible role of intra-agent speech in abstracting over time, and observing its effects on planning and reasoning.

Acknowledgments and Disclosure of Funding

The authors would like to thank Felix Hill and Nathaniel Wong for critical discussion and help with the development of scripted probe tasks, Chris Dyer and Daan Wierstra for reviewing and comments on the manuscript, and Alex Goldin and Guy Scully for organizational support.

References

- [1] Lev S Vygotsky. *Thought and language*. MIT press, 1934.
- [2] Adam Ed Winsler, Charles Ed Fernyhough, and Ignacio Ed Montero. *Private speech, executive functioning, and the development of verbal self-regulation*. Cambridge University Press, 2009.
- [3] Patti Adank, Peter Hagoort, and Harold Bekkering. Imitation improves language comprehension. *Psychological Science*, 21(12):1903–1909, 2010.
- [4] Conchi San Martín Martínez, Humbert Boada i Calbet, and Peter Feigenbaum. Private and inner speech and the regulation of social speech communication. *Cognitive Development*, 26(3): 214–229, 2011.
- [5] Alan D Baddeley, Susan E Gathercole, and Costanza Papagno. The phonological loop as a language learning device. *Exploring Working Memory*, pages 164–198, 2017.
- [6] Adam Winsler, Rafael M Diaz, and Ignacio Montero. The role of private speech in the transition from collaborative to independent task performance in young children. *Early Childhood Research Quarterly*, 12(1):59–79, 1997.
- [7] Ben Alderson-Day and Charles Fernyhough. Inner speech: development, cognitive functions, phenomenology, and neurobiology. *Psychological bulletin*, 141(5):931, 2015.
- [8] Alan D Baddeley. Short-term memory for word sequences as a function of acoustic, semantic and formal similarity. *Quarterly journal of experimental psychology*, 18(4):362–365, 1966.
- [9] Diane J Schiano and Michael J Watkins. Speech-like coding of pictures in short-term memory. *Memory & Cognition*, 9(1):110–114, 1981.
- [10] Antonis Hatzigeorgiadis, Nikos Zourbanos, Evangelos Galanis, and Yiannis Theodorakis. Self-talk and sports performance: A meta-analysis. *Perspectives on Psychological Science*, 6(4): 348–356, 2011.
- [11] Virginia S Tinsley and Harriet Salatas Waters. The development of verbal control over motor behavior: A replication and extension of luria’s findings. *Child Development*, pages 746–753, 1982.
- [12] Charles Fernyhough and Emma Fradley. Private speech on an executive task: Relations with task difficulty and task performance. *Cognitive development*, 20(1):103–120, 2005.
- [13] Durk P Kingma, Shakir Mohamed, Danilo Jimenez Rezende, and Max Welling. Semi-supervised learning with deep generative models. *Advances in neural information processing systems*, 27, 2014.
- [14] John Schulman, Xi Chen, and Pieter Abbeel. Equivalence between policy gradients and soft q-learning. *arXiv preprint arXiv:1704.06440*, 2017.
- [15] Sergey Levine. Reinforcement learning and control as probabilistic inference: Tutorial and review. *arXiv preprint arXiv:1805.00909*, 2018.
- [16] H Francis Song, Abbas Abdolmaleki, Jost Tobias Springenberg, Aidan Clark, Hubert Soyer, Jack W Rae, Seb Noury, Arun Ahuja, Siqi Liu, Dhruva Tirumala, et al. V-mpo: On-policy maximum a posteriori policy optimization for discrete and continuous control. *arXiv preprint arXiv:1909.12238*, 2019.
- [17] Aaron Van den Oord, Yazhe Li, and Oriol Vinyals. Representation learning with contrastive predictive coding. *arXiv e-prints*, pages arXiv–1807, 2018.
- [18] Aapo Hyvarinen and Hiroshi Morioka. Unsupervised feature extraction by time-contrastive learning and nonlinear ica. *Advances in Neural Information Processing Systems*, 29, 2016.
- [19] Chris Dyer. Notes on noise contrastive estimation and negative sampling. *arXiv preprint arXiv:1410.8251*, 2014.

- [20] Alec Radford, Jong Wook Kim, Chris Hallacy, Aditya Ramesh, Gabriel Goh, Sandhini Agarwal, Girish Sastry, Amanda Askell, Pamela Mishkin, Jack Clark, et al. Learning transferable visual models from natural language supervision. In *International Conference on Machine Learning*, pages 8748–8763. PMLR, 2021.
- [21] Chao Jia, Yinfei Yang, Ye Xia, Yi-Ting Chen, Zarana Parekh, Hieu Pham, Quoc Le, Yun-Hsuan Sung, Zhen Li, and Tom Duerig. Scaling up visual and vision-language representation learning with noisy text supervision. In *International Conference on Machine Learning*, pages 4904–4916. PMLR, 2021.
- [22] DeepMind Interactive Agents Team. Creating multimodal interactive agents with imitation and self-supervised learning. *arXiv preprint arXiv:2112.03763*, 2021.
- [23] Ashish Vaswani, Noam Shazeer, Niki Parmar, Jakob Uszkoreit, Llion Jones, Aidan N Gomez, Łukasz Kaiser, and Illia Polosukhin. Attention is all you need. *Advances in neural information processing systems*, 30, 2017.
- [24] Taku Kudo and John Richardson. Sentencepiece: A simple and language independent subword tokenizer and detokenizer for neural text processing. *arXiv preprint arXiv:1808.06226*, 2018.
- [25] Jack W Rae, Sebastian Borgeaud, Trevor Cai, Katie Millican, Jordan Hoffmann, Francis Song, John Aslanides, Sarah Henderson, Roman Ring, Susannah Young, et al. Scaling language models: Methods, analysis & insights from training gopher. *arXiv preprint arXiv:2112.11446*, 2021.
- [26] Aaron Van Den Oord, Oriol Vinyals, et al. Neural discrete representation learning. *Advances in neural information processing systems*, 30, 2017.
- [27] Zijun Zhang. Improved adam optimizer for deep neural networks. In *2018 IEEE/ACM 26th International Symposium on Quality of Service (IWQoS)*, pages 1–2. IEEE, 2018.
- [28] Google Cloud. Cloud tensor processing units (tpus), 2022. <https://cloud.google.com/tpu/docs/tpus> [Accessed: 2022-05-19].
- [29] Jean-Baptiste Alayrac, Adria Recasens, Rosalia Schneider, Relja Arandjelović, Jason Ramapuram, Jeffrey De Fauw, Lucas Smaira, Sander Dieleman, and Andrew Zisserman. Self-supervised multimodal versatile networks. *Advances in Neural Information Processing Systems*, 33:25–37, 2020.
- [30] Ramakrishna Vedantam, C Lawrence Zitnick, and Devi Parikh. Cider: Consensus-based image description evaluation. In *Proceedings of the IEEE conference on computer vision and pattern recognition*, pages 4566–4575, 2015.
- [31] Jared Kaplan, Sam McCandlish, Tom Henighan, Tom B Brown, Benjamin Chess, Rewon Child, Scott Gray, Alec Radford, Jeffrey Wu, and Dario Amodei. Scaling laws for neural language models. *arXiv preprint arXiv:2001.08361*, 2020.
- [32] Ali Razavi, Aaron Van den Oord, and Oriol Vinyals. Generating diverse high-fidelity images with vq-vae-2. *Advances in neural information processing systems*, 32, 2019.
- [33] Karl Moritz Hermann, Felix Hill, Simon Green, Fumin Wang, Ryan Faulkner, Hubert Soyer, David Szepesvari, Wojciech Marian Czarnecki, Max Jaderberg, Denis Teplyashin, et al. Grounded language learning in a simulated 3d world. *arXiv preprint arXiv:1706.06551*, 2017.
- [34] Maxime Chevalier-Boisvert, Dzmitry Bahdanau, Salem Lahlou, Lucas Willems, Chitwan Saharia, Thien Huu Nguyen, and Yoshua Bengio. Babyai: A platform to study the sample efficiency of grounded language learning. *arXiv preprint arXiv:1810.08272*, 2018.
- [35] Corey Lynch, Mohi Khansari, Ted Xiao, Vikash Kumar, Jonathan Tompson, Sergey Levine, and Pierre Sermanet. Learning latent plans from play. In *Conference on robot learning*, pages 1113–1132. PMLR, 2020.
- [36] Felix Hill, Sona Mokra, Nathaniel Wong, and Tim Harley. Human instruction-following with deep reinforcement learning via transfer-learning from text. *arXiv preprint arXiv:2005.09382*, 2020.

- [37] Ziad Al-Halah, Santhosh K Ramakrishnan, and Kristen Grauman. Zero experience required: Plug & play modular transfer learning for semantic visual navigation. *arXiv preprint arXiv:2202.02440*, 2022.
- [38] Suraj Nair, Eric Mitchell, Kevin Chen, Silvio Savarese, Chelsea Finn, et al. Learning language-conditioned robot behavior from offline data and crowd-sourced annotation. In *Conference on Robot Learning*, pages 1303–1315. PMLR, 2022.
- [39] Corey Lynch and Pierre Sermanet. Language conditioned imitation learning over unstructured data. *arXiv preprint arXiv:2005.07648*, 2020.
- [40] Eric Jang, Alex Irpan, Mohi Khansari, Daniel Kappler, Frederik Ebert, Corey Lynch, Sergey Levine, and Chelsea Finn. Bc-z: Zero-shot task generalization with robotic imitation learning. In *Conference on Robot Learning*, pages 991–1002. PMLR, 2022.
- [41] Hieu Pham, Zihang Dai, Golnaz Ghiasi, Hanxiao Liu, Adams Wei Yu, Minh-Thang Luong, Mingxing Tan, and Quoc V Le. Combined scaling for zero-shot transfer learning. *arXiv preprint arXiv:2111.10050*, 2021.
- [42] Laura Ruis, Jacob Andreas, Marco Baroni, Diane Bouchacourt, and Brenden M Lake. A benchmark for systematic generalization in grounded language understanding. *Advances in neural information processing systems*, 33:19861–19872, 2020.
- [43] Chelsea Finn, Tianhe Yu, Tianhao Zhang, Pieter Abbeel, and Sergey Levine. One-shot visual imitation learning via meta-learning. In *Conference on robot learning*, pages 357–368. PMLR, 2017.
- [44] Yan Duan, Marcin Andrychowicz, Bradly Stadie, OpenAI Jonathan Ho, Jonas Schneider, Ilya Sutskever, Pieter Abbeel, and Wojciech Zaremba. One-shot imitation learning. *Advances in neural information processing systems*, 30, 2017.
- [45] Allan Zhou, Eric Jang, Daniel Kappler, Alex Herzog, Mohi Khansari, Paul Wohlhart, Yunfei Bai, Mrinal Kalakrishnan, Sergey Levine, and Chelsea Finn. Watch, try, learn: Meta-learning from demonstrations and reward. *arXiv preprint arXiv:1906.03352*, 2019.
- [46] Kourosh Hakhmaneshi, Ruihan Zhao, Albert Zhan, Pieter Abbeel, and Michael Laskin. Hierarchical few-shot imitation with skill transition models. *arXiv preprint arXiv:2107.08981*, 2021.
- [47] Yishu Miao and Phil Blunsom. Language as a latent variable: Discrete generative models for sentence compression. *arXiv preprint arXiv:1609.07317*, 2016.
- [48] Jason Lee, Kyunghyun Cho, and Douwe Kiela. Countering language drift via visual grounding. *arXiv preprint arXiv:1909.04499*, 2019.
- [49] Angeliki Lazaridou, Anna Potapenko, and Olivier Tieleman. Multi-agent communication meets natural language: Synergies between functional and structural language learning. *arXiv preprint arXiv:2005.07064*, 2020.
- [50] Wenhui Chen, Aurelien Lucchi, and Thomas Hofmann. A semi-supervised framework for image captioning. *arXiv preprint arXiv:1611.05321*, 2016.
- [51] Bicheng Xu, Weirui Kong, and Jiaxuan Chen. Semi-supervised image captioning via reconstruction. In *Proceedings of the Intern. Conf. on Comp. Vis.(ICCV)*, pages 4135–4144, 2017.
- [52] Dong-Jin Kim, Jinsoo Choi, Tae-Hyun Oh, and In So Kweon. Image captioning with very scarce supervised data: Adversarial semi-supervised learning approach. *arXiv preprint arXiv:1909.02201*, 2019.
- [53] Jonathan Ho, Ajay Jain, and Pieter Abbeel. Denoising diffusion probabilistic models. *Advances in Neural Information Processing Systems*, 33:6840–6851, 2020.
- [54] Jascha Sohl-Dickstein, Eric Weiss, Niru Maheswaranathan, and Surya Ganguli. Deep unsupervised learning using nonequilibrium thermodynamics. In *International Conference on Machine Learning*, pages 2256–2265. PMLR, 2015.

- [55] Yang Song and Stefano Ermon. Improved techniques for training score-based generative models. *Advances in neural information processing systems*, 33:12438–12448, 2020.
- [56] Aditya Ramesh, Mikhail Pavlov, Gabriel Goh, Scott Gray, Chelsea Voss, Alec Radford, Mark Chen, and Ilya Sutskever. Zero-shot text-to-image generation. In *International Conference on Machine Learning*, pages 8821–8831. PMLR, 2021.
- [57] Aditya Ramesh, Prafulla Dhariwal, Alex Nichol, Casey Chu, and Mark Chen. Hierarchical text-conditional image generation with clip latents. *arXiv preprint arXiv:2204.06125*, 2022.
- [58] Alex Nichol, Prafulla Dhariwal, Aditya Ramesh, Pranav Shyam, Pamela Mishkin, Bob McGrew, Ilya Sutskever, and Mark Chen. Glide: Towards photorealistic image generation and editing with text-guided diffusion models. *arXiv preprint arXiv:2112.10741*, 2021.
- [59] Tiago Ramalho, Tomáš Kočiský, Frederic Besse, SM Eslami, Gábor Melis, Fabio Viola, Phil Blunsom, and Karl Moritz Hermann. Encoding spatial relations from natural language. *arXiv preprint arXiv:1807.01670*, 2018.
- [60] Scott Reed, Zeynep Akata, Xinchun Yan, Lajanugen Logeswaran, Bernt Schiele, and Honglak Lee. Generative adversarial text to image synthesis. In *International conference on machine learning*, pages 1060–1069. PMLR, 2016.
- [61] Tao Xu, Pengchuan Zhang, Qiuyuan Huang, Han Zhang, Zhe Gan, Xiaolei Huang, and Xiaodong He. Attngan: Fine-grained text to image generation with attentional generative adversarial networks. In *Proceedings of the IEEE conference on computer vision and pattern recognition*, pages 1316–1324, 2018.
- [62] Minfeng Zhu, Pingbo Pan, Wei Chen, and Yi Yang. Dm-gan: Dynamic memory generative adversarial networks for text-to-image synthesis. In *Proceedings of the IEEE/CVF Conference on Computer Vision and Pattern Recognition*, pages 5802–5810, 2019.
- [63] Han Zhang, Jing Yu Koh, Jason Baldridge, Honglak Lee, and Yinfei Yang. Cross-modal contrastive learning for text-to-image generation. In *Proceedings of the IEEE/CVF Conference on Computer Vision and Pattern Recognition*, pages 833–842, 2021.
- [64] Hui Ye, Xiulong Yang, Martin Takac, Rajshekhar Sunderraman, and Shihao Ji. Improving text-to-image synthesis using contrastive learning. *arXiv preprint arXiv:2107.02423*, 2021.

A Appendix

A.1 Contrastive cross-entropy approximates generative log-likelihood

Consider a batch of images $\{\mathbf{x}_b\}_{b=1}^B$ and a caption \mathbf{y} corresponding to one of the images \mathbf{x}_j . This caption will come either from the paired dataset or as a sample from the image-conditional language encoder $q_\omega(\mathbf{y} | \mathbf{x}_j)$.

The posterior distribution over the classification of the image index c is

$$\Pr(c = j | \{\mathbf{x}_b\}_{b=1}^B, \mathbf{y}) = \frac{p(\mathbf{x}_j | \mathbf{y}) \prod_{i \neq j} p(\mathbf{x}_i)}{\sum_b p(\mathbf{x}_b | \mathbf{y}) \prod_{k \neq b} p(\mathbf{x}_k)} = \frac{p(\mathbf{x}_j | \mathbf{y})/p(\mathbf{x}_j)}{\sum_b p(\mathbf{x}_b | \mathbf{y})/p(\mathbf{x}_b)}. \quad (8)$$

Therefore, the multi-class cross-entropy over the correct index is

$$L(\{\mathbf{x}_b\}_{b=1}^B, \mathbf{y}, c = j) = \log p(\mathbf{x}_j | \mathbf{y}) - \log p(\mathbf{x}_j) - \log \sum_b \frac{p(\mathbf{x}_b | \mathbf{y})}{p(\mathbf{x}_b)}. \quad (9)$$

We can manipulate the third term into the form of an expectation

$$L(\{\mathbf{x}_b\}_{b=1}^B, \mathbf{y}, c = j) = \log p(\mathbf{x}_j | \mathbf{y}) - \log p(\mathbf{x}_j) - \log \frac{1}{B} \sum_b \frac{p(\mathbf{x}_b | \mathbf{y})}{p(\mathbf{x}_b)} - \log B, \quad (10)$$

and for large B , we can approximate $\frac{1}{B} \sum_b \frac{p(\mathbf{x}_b | \mathbf{y})}{p(\mathbf{x}_b)} \approx \mathbb{E}_{p(\mathbf{x})} \left[\frac{p(\mathbf{x} | \mathbf{y})}{p(\mathbf{x})} \right] = \int_{\mathbf{x}} p(\mathbf{x} | \mathbf{y}) = 1$. In this large batch limit, the multi-class cross-entropy is proportional to the language-conditional image decoder log-likelihood up to constant factors in \mathbf{y} :

$$L(\{\mathbf{x}_b\}_{b=1}^B, \mathbf{y}, c = j) \approx \log p(\mathbf{x}_j | \mathbf{y}) + \text{constant}(\mathbf{y}). \quad (11)$$

Therefore, if we have a multi-class classifier that discriminates if a batch element \mathbf{y} is paired to a batch element \mathbf{x} , we can substitute the generative log likelihood with the classifier's loss:

$$\mathbb{E}_{q_\omega(\mathbf{y} | \mathbf{x}_j)} [\log p_\theta(\mathbf{x}_j | \mathbf{y})] = \mathbb{E}_{q_\omega(\mathbf{y} | \mathbf{x}_j)} [L(\{\mathbf{x}_b\}_{b=1}^B, \mathbf{y}, c = j)] + \text{constant}(\mathbf{y}), \quad (12)$$

and gradients with respect to $q_\omega(\mathbf{y} | \mathbf{x}_j)$ are the same in expectation.

A.2 Details for caption data collection

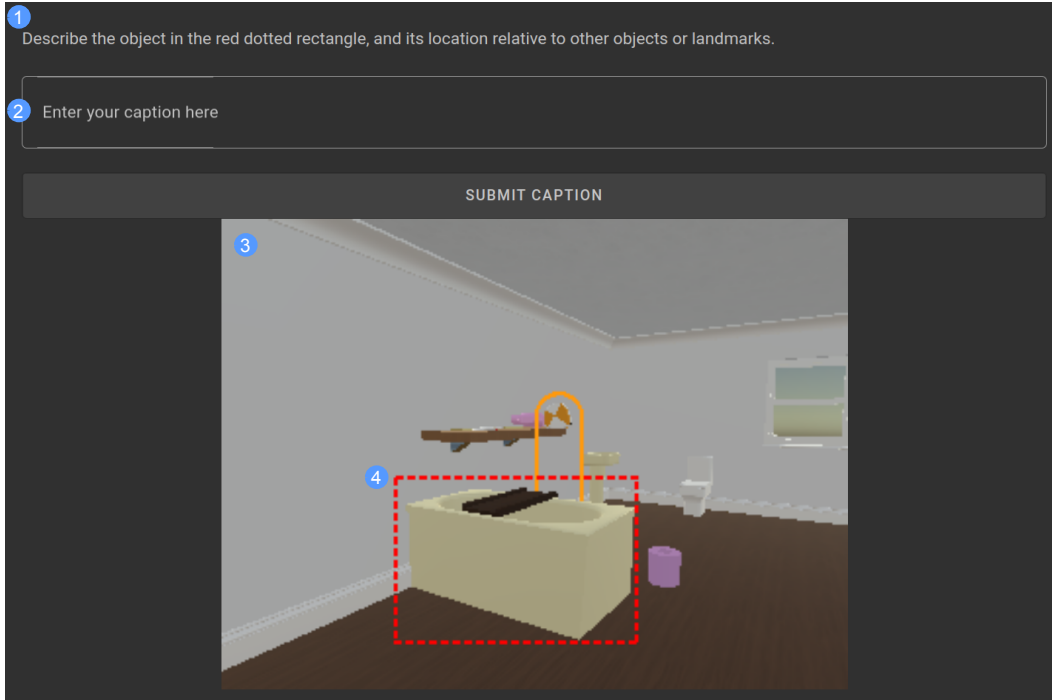


Figure A1: User interface and instructions for caption data collection. We recruited participants ($N = 80$) through an internal crowdsourcing pool, and collected a total of 78K captions using a total of 4,000 participant hours. The full details of our study design, including compensation rates, were reviewed by our institution’s independent ethical review committee. All participants provided informed consent prior to completing tasks and were reimbursed for their time. Participants were provided with a link to the caption interface and the following task description:

You will be shown an image of a room, where one of the objects is highlighted with a **dotted red rectangle**. Follow the script, think of a description of the **object and its surroundings** and type it in the text field. The description should have enough details such that another player in the room can easily find and understand which object you are referring to.

During data collection, the caption interface displayed a single frame randomly selected from human-human interaction data as described by [22] at a resolution of 320×240 . An object from the image was randomly selected and highlighted by a bounding box. The participants were prompted to “[d]escribe the object in the red dotted rectangle, and its location relative to other objects or landmarks”. After the participants input the caption in the text-box and clicked “submit”, the image is refreshed and text-box is cleared for the collection of next caption. *Numbered elements in caption interface:* 1. The prompt for the participants. 2. The text-box for the participants to input caption. 3. Image to be captioned. 4. Highlighted object in the scene.

A.3 Additional samples from generative semi-supervised model

Caption samples

Human: i can see one orange color helicopter near the green bus.

Model: i can see a green car on the floor which is near the brown helicopter



Human: there is a ledge below another ledge

Model: i can see a yellow duck on the green bed.



Human: on top of the wooden rack there is a green robot and a yellow lamp. under the wooden rack there is a violet lamp.

Model: i can see a wooden shelf at the wall.



Human: there is a cyan stool near two yellow objects

Model: i can see a blue frame on the floor which is near the window.



Human: the bed is in pink color, and in rectangular shape which is placed on the floor.

Model: i can see a olive green color car on the pink color bed near the three objects on it.



Human: i can see a violet color table and white ball on it, on the left there is a green bed, teddy on floor.

Model: i can see a green bed placed on floor and there is a teddy placed in front of that bed.



Human: there is a green rocket in front of the orange wardrobe, close to the bed.

Model: i can see a brown shelf, which is above the violet bed.



Human: there is a green engine on the floor which is in between the red headset and pink chopper.

Model: i can see a cyan headphone placed on floor and there is a bed placed near that headphone.



Language conditioned image samples

Human: i can see a orange color table on floor and a green color object is present.



Human: there is a yellow table, which is in front of the white lamp.



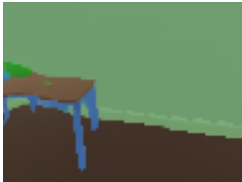
Human: there is a red color rack right of the brown color shelf



Human: there is a pink headphone on the floor which is near a green mug and a red headphone



Human: i can see blue table on which red hair dryer is placed



Human: there is a white box close to the green chair and green stool, in front of it we can see red headset and red car.



Human: i can see a pink color cupboard on top of the floor which is close to the wall.



Human: i can see a shelf under which there is another shelf and also i can see a shelf on which there are some objects placed.



Figure A2: Additional caption and image samples from generative semi-supervised model.

A.4 Details about lift / ask color tasks

We modified the Playhouse environment [22] to create the lift drum and ask color drum tasks. These tasks were used for evaluation only, and the agent was never trained in these tasks. For these tasks, We first initialize a randomized playhouse environment as described in [22], which represents a randomized multi-room environment. We then spawn a drum object in the room where the agent avatar is spawned. The color of the drum object is randomly selected from the following list of 10 colors: “red”, “yellow”, “blue”, “white”, “green”, “pink”, “purple”, “orange”, “aquamarine”, “magenta”.

Lift task. In the lift task, the instruction “Lift the drum.” appears after a random delay of up to 10 seconds. A reward of 1 is given if the agent lifts any drum object, and the episode terminates after reward is emitted. If the agent lifts any other object, or times out after 2 minutes, the episode terminates with a reward of 0.

Ask about color task. In the ask about color task, the instruction “What is the color of the drum?” appears after a random delay of up to 10 seconds. If the agent emits language that matches the color of the drum, a reward of 1 is given, and the episode terminates. Otherwise if the agent outputs any other text, or times out after 2 minutes with no language output, the episode terminates with a reward of 0.

For each agent, we averaged rewards collected from 1,000 episodes for each task. We also collected human scores on these tasks, and used it to normalize the agent reward to a range of [0, 1]. The human normalized score is reported in the manuscript.

A.5 Results on control objects

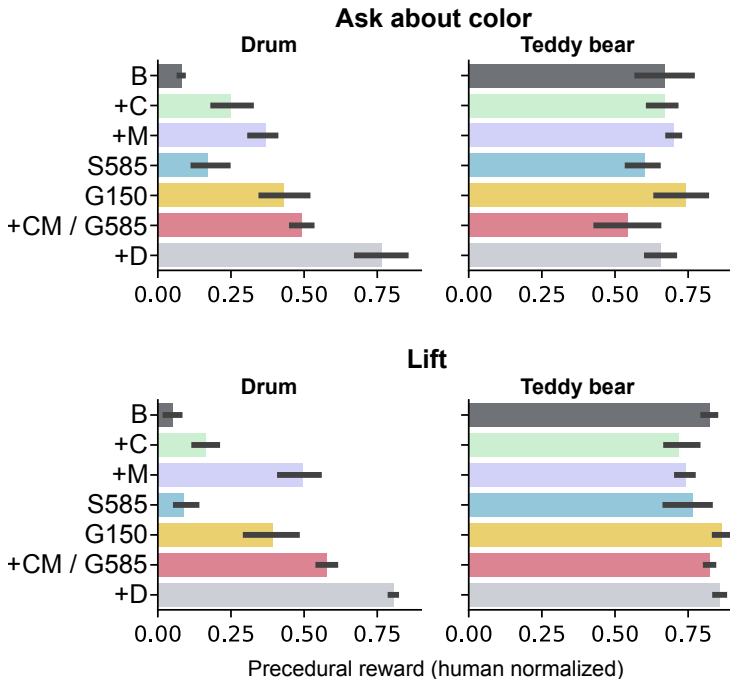


Figure A3: Performance on manipulating a control object. To confirm the improvement of performance on the drum task is a result of zero-shot generalization from drum captions without affecting the background ability of the agent, we tested the agent on the tasks targeting a control object, the teddy bear. The teddy bear object is included in the background interaction data and the agent has been trained on data manipulating teddy bear. These tasks are similar to the lift and ask about color tasks described in Appendix A.4, except that the drum object is replaced with the teddy bear object, and all instance of the word “drum” in the instructions are replaced with “teddy bear”. We show that the performance of these task is not different between different task, suggesting that our method of zero-shot learning new object does not affect background ability of the agent.